

Shock Waves in Nanomechanical Resonators

Florian W. Beil

*Center for NanoScience and Sektion Physik,
Ludwigs-Maximilians-Universität-München,
Geschwister-Scholl-Platz 1, 80539 München, Germany.*

Achim Wixforth

*Lehrstuhl für Experimentalphysik I, Universität Augsburg,
Universitätsstraße 1, D-86135 Augsburg, Germany.*

Werner Wegscheider and Dieter Schuh

*Institut für Angewandte und Experimentelle Physik,
Universität Regensburg, 93040 Regensburg, Germany.*

Max Bichler

Walter Schottky Institut, Am Coloumbwall 3, 85748 Garching, Germany.

Robert H. Blick*

*Electrical and Computer Engineering, University of Wisconsin-Madison,
1415 Engineering Drive, Madison WI 53706, USA.*

(Dated: August 10, 2021)

Abstract

The dream of every surfer is an extremely steep wave propagating at the highest speed possible. The best waves for this would be shock waves, but are very hard to surf. In the nanoscopic world the same is true: the surfers in this case are electrons riding through nanomechanical devices on acoustic waves [1]. Naturally, this has a broad range of applications in sensor technology and for communication electronics for which the combination of an electronic and a mechanical degree of freedom is essential. But this is also of interest for fundamental aspects of nano-electromechanical systems (NEMS), when it comes to quantum limited displacement detection [2] and the control of phonon number states [3]. Here, we study the formation of shock waves in a NEMS resonator with an embedded two-dimensional electron gas using surface acoustic waves. The mechanical displacement of the nano-resonator is read out via the induced acoustoelectric current. Applying acoustical standing waves we are able to determine the anomalous acoustocurrent. This current is only found in the regime of shock wave formation. We obtain very good agreement with model calculations.

PACS numbers: 73.50.Rb, 63.20.Kr

*Electronic address: blick@engr.wisc.edu

Over the past two decades a multitude of work focused on reducing the dimensionality of electronic systems from three to zero dimensions, leading to extremely interesting physics [4]. Only recently the availability of even more intricate nano-structuring techniques made it possible to morph the dimensionality of the phonon systems, i.e. to construct phonon cavities with nano-scale dimensions. An example of this are freely suspended two-dimensional electron systems (2DEG), for which the phonon modes can be tailored [5]. The combination of low-dimensional electron gases and nanomechanical systems is interesting for several reasons: the most obvious being the ability to study intricate effects of the electron-phonon interaction. In other words dissipation in the limit of single electrons interacting with discrete phonon modes [6]. This is revealed in the formation of van Hove-singularities in the phonon density of states for low-dimensional phonon systems [7]. Furthermore, suspended 2DEGs, quantum wires, and quantum dots, are the perfect tools for studying quantum electromechanical (QEM) effects [8] and might further improve measurements for the current standard [9].

The main limitation encountered so far is the fact that the phonon system, in contrast to the electronic one, could not be actuated directly. Nevertheless, the method of choice for generating such an acoustic actuation is readily available: surface acoustic waves (SAW) are a proven tool for investigating non-suspended 2DEGs already [10]. Hence, we set out to combine low-dimensional electron systems embedded in a nanomechanical resonator with SAW generators, such as interdigitated transducers (IDTs). In early work we demonstrated how to achieve acoustical coupling of an ordinary nanomechanical resonator (suspended beam without electron gas) to SAWs [11] and were able to show how acoustical standing wave patterns can be detected in such a resonator [12]. Recently, we pushed the resolution of these measurements and were able to resolve single defect relaxation [13] and phonon population inversion in a nano-resonator [14].

In this Letter we present acoustical excitation of a nano-resonator with an integrated 2DEG by SAW, leading to the formation of shock waves in the nanomechanical system. Shock wave formation is probed with the help of the so-called anomalous acoustoelectric effect, one of the manifestations of the electron-phonon interaction. Acoustoelectric effects have up to now been mainly studied in quantum wells, where the mechanical properties are determined by the bulk [10, 15]. It is apparent that the investigation of acoustoelectric effects in low dimensional mechanical systems is also interesting for improving current standards [9, 16, 17] and elucidate effects like the anomalous acoustoelectric effect observed in thin films

itself [18]. The reasoning is straight forward: suspending low-dimensional electron systems leads to giant displacements as compared to SAWs on bulk, hence, the interaction of electrons and acoustical phonons is extremely enhanced.

In the following we will describe how SAWs mechanically excite the suspended electronic specimen and how acoustic currents are observed. The measured current consists of two components, of which one is an anomalous current. This current directly traces the shock wave formation in the nano-resonator. As shock wave we define the transition from a linear response such as a sinusoidal excitation towards nonlinear wave forms of the nano-resonator's displacement.

Methods– The processing follows standard techniques for suspended 2DEGs [19, 20], with the difference that we integrate interdigitated transducers (IDTs) for SAW generation on the sample. Starting with an AlGaAs-heterostructure containing a 2DEG grown above a sacrificial layer (300 nm thickness), the freely suspended electronic system is defined by successive lithography steps. The lateral structures of the suspended 2DEGs and the IDTs are then defined via electron beam lithography. In a further step, anisotropic reactive ion etching (RIE) is applied to mill out the lithographically defined structure. Finally, the sacrificial layer is removed in an isotropic wet etch step with hydrofluoric acid. In Fig. 1 a scanning electron micrograph of the sample is shown. The inset presents the suspended beam of length $L = 1.2 \mu\text{m}$, width $w = 300 \text{ nm}$, and height $h = 200 \text{ nm}$ used in the experiments. As seen the suspended sample is placed between two IDTs forming an acoustic delay line. In the following the two IDTs are excited with continuous waves from two synthesizers.

For the first set of experiments we generate the acoustical waves in one transducer, while for shock wave probing we couple both IDTs to generate an acoustical standing wave pattern and then trace the induced direct current. The transducers generate a coherent acoustic sound wave via the inverse piezo effect, at the lithographically defined center frequency f_{saw} . This corresponds to a SAW wavelength $\lambda_{\text{saw}} = 7 \mu\text{m}$ resp. $9 \mu\text{m}$. The SAW frequency and wavelength are connected via $f_{\text{saw}} = v_{\text{saw}}/\lambda_{\text{saw}}$, where $v_{\text{saw}} = 2865 \text{ m/s}$ is the surface wave velocity on GaAs in the [011]-direction. It has to be noted that no acoustic power is reflected at the etch boundaries produced by the anisotropic RIE step, due to the small height compared to the SAW wavelength. In order to measure the acoustoelectric effects in the 2DEG in a two point fashion, we either employ a lock-in technique (as demonstrated in Fig. 1), or measure the direct current driven through the 2DEG with an optional DC bias

voltage. Thus both the resistance of the beam and the direct current can be measured in dependence of acoustic wave excitation.

Experiment– For determining the quality of the suspended electron system we first took magnetoresistance traces of the freely suspended 2DEG at 100 mK (Fig. 2(a)). The longitudinal resistance exhibits $1/B$ periodic Shubnikov-de Haas oscillations, from which we calculate a carrier density of $6.56 \times 10^{15} \text{ m}^{-2}$ with a mobility of $\mu = 3057 \text{ cm}^2 /(\text{Vs})$. The peak in the resistance at low magnetic field (cf. inset of Fig. 2(a)) is due to coherent back scattering effects in the suspended 2DEG, as discussed elsewhere [19]. A backgate voltage V_{bg} is applied to alter the suspended 2DEG’s resistance. In Fig. 2(b) we show the effect of acoustic excitation by the left and right IDT firing at the suspended beam. Scanning the radio frequency signal applied at the left IDT results in a modulation of the current which can be passed through the sample. A notable current modulation is only observed when f is approximately f_{SAW} and a maximal acoustic power is generated.

In detail, the induced acoustoelectric current is depicted when either the left or the right IDT are driven by one of the synthesizers. While the left transducer generates a forward current the right one reverses the current direction and pumps electrons backwards. These traces are recorded under increasing RF power (0 dBm ... +10 dBm). The dependence of the SAW induced current on IDT-frequency f , SAW power and propagation direction are consistent with previous measurements of the acoustoelectrical current in non-suspended 2DEGs [16] and quantum point contacts [17]. The amplitude of the normal acoustoelectric current is given by $I_n = ne f_{\text{SAW}}$, where n is the integer number of electrons transferred: this suggests that during each SAW cycle ~ 380 electrons are transferred through the suspended 2DEG.

In addition to this conventional acoustoelectric current a peculiar feature appears in Fig. 2(b) at the left edge of the IDTs’ main transmission centered at 350 MHz: the acoustic current in the shoulder of the current peak is caused by an additional current that is *not* changing sign with SAW direction. This so-called *anomalous acoustoelectric* current I_{an} was first observed in thin manganite films [18] and was explained by the elastic deformation of the thin film by the SAW. The resulting unidirectional current (I_{an}) is found to be even in the SAW wave vector k_{SAW} , and thus invariant under inversion of SAW direction. The total acoustoelectric current then is given as a superposition of the normal and anomalous components $I_n + I_{\text{an}}$.

It is this anomalous acoustoelectric current, which allows us to probe the deformation of the nanomechanical device directly. In order to read out the unidirectional current we conducted acoustic standing wave experiments: a standing wave is formed by applying phase locked RF-signals to both IDTs, left and right of the sample. Shifting the relative phase ϕ of the driving signal at one IDT with respect to the other results in a lateral shift of the standing wave pattern. If a perfect standing wave is formed the total wave vector equals to zero and the only contribution to the measured acoustoelectric current is the anomalous component I_{an} . *In other words the normal acoustoelectric current depends only on the propagating part, whereas the anomalous current depends on the mechanical deformation induced in the suspended 2DEG.* Thus we have a direct relation between the mechanical deformation and the relative phase ϕ , which allows us to map the mechanical mode of the suspended beam.

In Fig. 3(a) the standing wave pattern of the anomalous current is shown: evidently the initial trace with moderate power levels applied to the IDTs is a fundamental mode of the suspended nanomechanical device, forming a sinusoidal-trace. Increasing the acoustic power leads to a larger current, i.e. the trace is increased towards more negative currents. Evidently, the shape of the standing wave pattern is changed once the relative phase ϕ of the two synthesizers is altered. The deviation from the sinusoidal-waveform shows up as a pronounced peak around $\phi = 180$ deg. This is the transition from linear to nonlinear response, where the steepening of the trace indicates *shock wave formation*. In other words, all of the energy of the SAW is compressed around $\phi = 180$ deg, resulting in this nonlinear wave form. By varying ϕ , we shift the maxima and minima of the acoustic wave through the resonator, thus mapping the deformation of the resonator directly in the current response. In Fig. 3(b) the standing wave pattern of the anomalous current is shown for even larger acoustic excitation power levels: the shock wave form now develops extremely high current levels around $\phi = 0$ deg and 360 deg. A pronounced peak at $\phi = 180$ deg is accompanied by two apparent shoulders to its left and right. For the highest power levels shown in the figure, the 'wave form' returns to one resembling a sinusoidal again. We interpret this as the final transition into a higher order mode.

Theory – In Fig. 4(a) we show the full power dependence of the acoustic current while altering ϕ from smallest to largest driving powers at the IDTs. As seen the ground mode shows a slight sinusoidal-modulation, which deforms into a shock wave, indicated by the sharp peak and the two shoulders discussed above at intermediate power levels. A further

increase in power switches the system to the next higher mode, which again shows a sinusoidal wave form response. Evidently, this series of traces depicts a transition from the first fundamental mode to the next higher mode with a larger current amplitude.

To model this effect we calculated the anomalous acoustoelectric current in the suspended 2DEG, induced by altering the phase shift of the acoustic standing wave, following Illisavskii *et al.* [18]. When an acoustic wave interacts with a thin film, the induced mechanical strain modulates the local conductivity, which induces an acoustoelectric current density j per unit length

$$j(z) = \frac{a \omega}{2\pi} \int_0^{\frac{2\pi}{\omega}} \sigma_{zz}(z, t) E_z(z, t) dt, \quad (1)$$

where ω is the SAW frequency, a the thickness of the resonator, σ_{zz} is the component of the conductivity tensor along the z -axes (the [110] direction, cf. Fig. 1), and E_z is the electric field along z . Eq. (1) neglects any dependence on the y -coordinate, which is justified due to the 'thinness' of the sample of only 200 nm, compared to its length of $\sim 1 \mu\text{m}$. The SAW induced strain in the beam S_{ij} will modulate the conductivity following

$$\begin{aligned} \sigma_{zz}(z, t) = \sigma_0(\Pi_{zzzz}S_{zz}(z, t) + \Pi_{zzyy}S_{yy}(z, t) + \\ \Pi_{zzzy}S_{yz}(z, t)), \end{aligned} \quad (2)$$

where σ_0 is the unperturbed conductivity, and the tensor Π_{ijkl} describes the effect of strain S_{jk} on the conductivity σ_{ik} and evaluates to $\Pi_{ijkl} = \delta\sigma_{ij}/\delta S_{jk}$. To solve Eq. (1) in combination with Eq. (2) we have to determine the SAW induced strain in the beam and relate it to E_z . If two counter propagating SAWs form a standing wave pattern, the motion of the clamping points will induce stress in the beam, extending from 0 to L in the z -direction, which is calculated to [13]

$$\begin{aligned} S_{zz}(z, t) &= \frac{2A_l(\cos(\phi/2) + \cos(k_{\text{saw}}L + \phi/2))}{L}, \\ S_{zy}(z, t) &= 2A_t\left(\frac{6z^2}{L^3} - \frac{6z}{L^2}\right)(\cos(\phi/2) - \\ &\quad \cos(k_{\text{saw}}L + \phi/2)), \end{aligned} \quad (3)$$

where A_t resp. A_l are the transversal respectively longitudinal components of the SAW motion, and L is the length of the beam. The relation between the strain and the electric field is found in the piezoelectric constitutive relation $D_z = \epsilon_{\text{GaAs}}E_z + e_{z4}S_{zy}$, where D_z is the electric displacement in z direction, ϵ_{GaAs} is the dielectric constant of GaAs, and e_{z4}

is the appropriate constant of the piezoelectric tensor, which has to be taken in the [110] coordinate system. This can be solved for E_z to give

$$E_z(z, t) = -\frac{e_{z4}}{\epsilon_{\text{GaAs}}} S_{zy}, \quad (4)$$

where the contribution of D_z was neglected. This is justified if $1 \ll \sigma_0/\epsilon_{\text{GaAs}}\omega \ll 1/\lambda_D k_{\text{saw}}$, where λ_D is the Debye length [18]. In our case $\sigma_0/\epsilon_{\text{GaAs}}\omega \sim 10^6$ and the condition for disregarding D_z is fulfilled. From Eq. (1-4) the current density due to the anomalous acoustoelectric effect in the center of the beam $z = L/2$ calculates to

$$j_{an}(L/2) = -\frac{\sigma_0 e_{z4}}{2 \epsilon_{\text{GaAs}}} (\Pi_{zzzy} S_{zy}(L/2)^2), \quad (5)$$

where the mixed term S_{zz} , S_{xy} in Eq. (1) equals to 0, when integrated over one SAW period as the longitudinal and transversal SAW component are $\pi/2$ phase shifted in time. The calculated current in dependence on ϕ is shown in the inset of Fig. 4(b). Eq. 5 predicts a square dependence of the anomalous acoustoelectric current on the SAW amplitude. Using the measured input impedances of the two IDTs it is possible to convert the RF power applied at the transducers into an estimate for the amplitude of the excited SAW [13]. Finally, in Fig. 4(b) shows the maximum of the anomalous acoustoelectric current component plotted vs. applied SAW amplitude. The curve follows the predicted behavior for not too small SAW amplitudes, which can be evaluated by fitting this section [cf. Fig. 4(b)]. The exponent we extract from this fit evaluates to 2.06 ± 0.3 , which is in very good agreement with the expected value. From this fit we further estimate the size of Π_{zzzy} to be on the order of 10^5 , which is *one order of magnitude larger* than observed for thin manganite films [18]. The minor deviations of the induced current for small SAW amplitudes suggests that the linear dependence of conductivity on strain might be an over-simplification. This can be due to different contributions like dislocations [13] or band deformation [21].

Conclusion– In summary we have shown that shock waves can be generated in nanomechanical resonators. The resonators contain an electron gas, which we apply to probe the shock waves via the acoustoelectric effect. This observation is explained by the presence of two current components, the normal and the anomalous current. The anomalous acoustoelectric current is mediated via the strain modulated conductivity in the suspended 2DEG and is described by model calculations. The results will have wide spread use for quantum electromechanics (QEM), as well as for applications in sensor and communication electronics.

Acknowledgements— We thank J.P. Kotthaus and M.L. Roukes for helpful discussions and support. We acknowledge support in part by the Deutsche Forschungsgemeinschaft under contract number Bl-487/3, the Air Force OSR (F49620-03-1-0420), the Graduate School of the University of Wisconsin, and the National Science Foundation (NSF-NIRT).

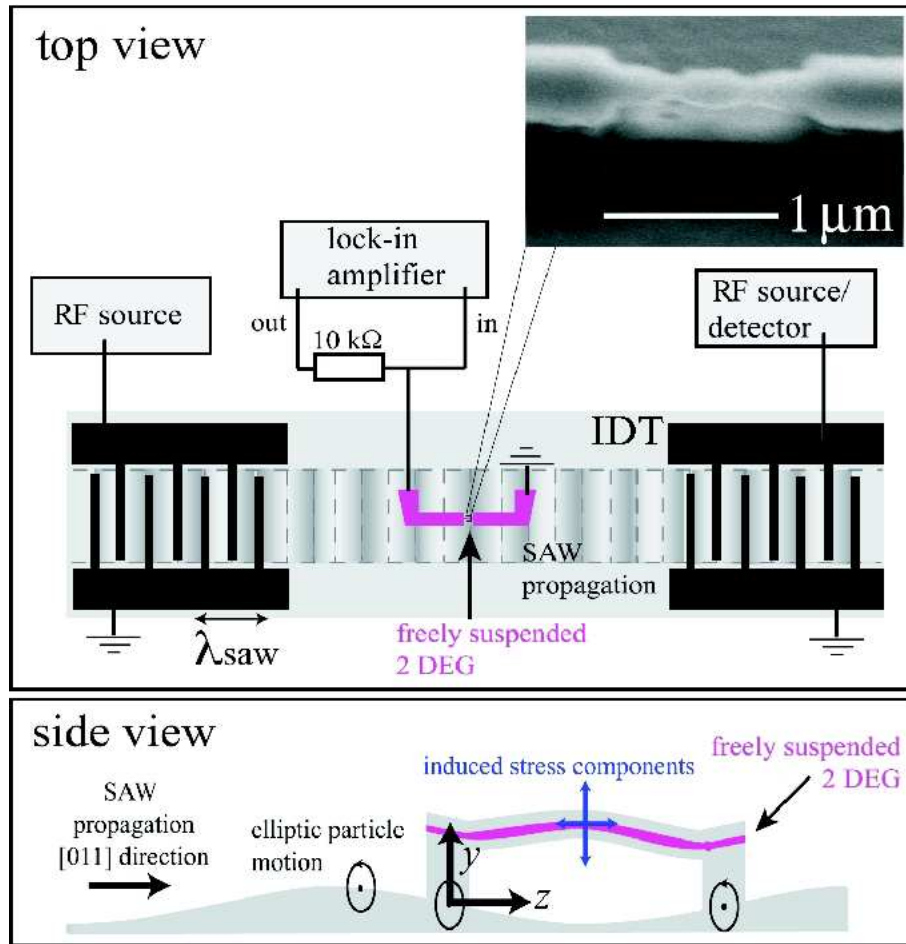
- [1] S. Zimmermann *et al.*, *Science* **283**, 1292-1294 (1999).
- [2] R.G. Knobel and A.N. Cleland, *Nature* **424**, 291-293 (2003).
- [3] M.D. LaHaye *et al.*, *Science* **304**, 74-77 (2006).
- [4] J.H. Davies, *The Physics of Low-Dimensional Electron Systems: An Introduction*, Cambridge University Press (1998).
- [5] R.H. Blick *et al.*, *Phys. Rev. B* **62**, 17103-17105 (2000).
- [6] E.M. Weig *et al.*, *Phys. Rev. Lett.* **92**, 046804-046807 (2004).
- [7] S. DeBald, T. Brandes, and B. Kramer, *Phys. Rev. B* **66**, 041301-041307 (2002).
- [8] M. Blencowe, *Phys. Rep.* **395**, 159-171 (2004).
- [9] M.D. Blumenthal *et al.*, *Nature Physics* **3**, 343-347 (2007).
- [10] A. Wixforth *et al.*, *Phys. Rev. B* **40**, 7874-7879 (1989).
- [11] F.W. Beil, A. Wixforth, and R.H. Blick, *Proceedings of IEEE Sensors* **1**, 1285-1289 (2002).
- [12] F. W. Beil, R. H. Blick, and A. Wixforth, *Physica E* **21**, 1106-1108 (2004).
- [13] F.W. Beil *et al.*, *Europhys. Lett.* **76**, 1207-1211 (2006).
- [14] F.W. Beil *et al.*, *Appl. Phys. Lett.* **90**, 043101-04103 (2007).
- [15] A.O. Govorov *et al.*, *Phys. Rev. B* **62**, 2659-2663 (2000).
- [16] J.M. Shilton *et al.*, *J. Phys.: Condens Matter* **8**, L531-L539 (1996).
- [17] V.I. Talyanskii *et al.*, *Phys. Rev. B* **56**, 15180-15186 (1997).
- [18] Y. Ilisavskii *et al.*, *Phys. Rev. Lett.* **87**, 146602-146605 (2001).
- [19] J. Kirschbaum *et al.*, *Appl. Phys. Lett.* **81**, 280-282 (2002).
- [20] E.M. Höhberger *et al.*, *Appl. Phys. Lett.* **82**, 4160-4162 (2003).
- [21] C. Jagannath *et al.*, *Phys. Rev. Rev. B* **34**, 7027-7032 (1986).

FIG. 1: Top and side view of the sample geometry and experimental setup. The top part contains a micrograph of the sample, which shows the suspended specimen placed in the delayline formed by two IDTs. Inset gives a scanning electron microscope picture of the device. The electron gas is confined in the 100 nm thin membrane. The freely suspended 2DEG interacts with the travelling SAW via the elliptic motion of clamping points. This mechanical excitation induces acoustoelectric currents measured in the direct current.

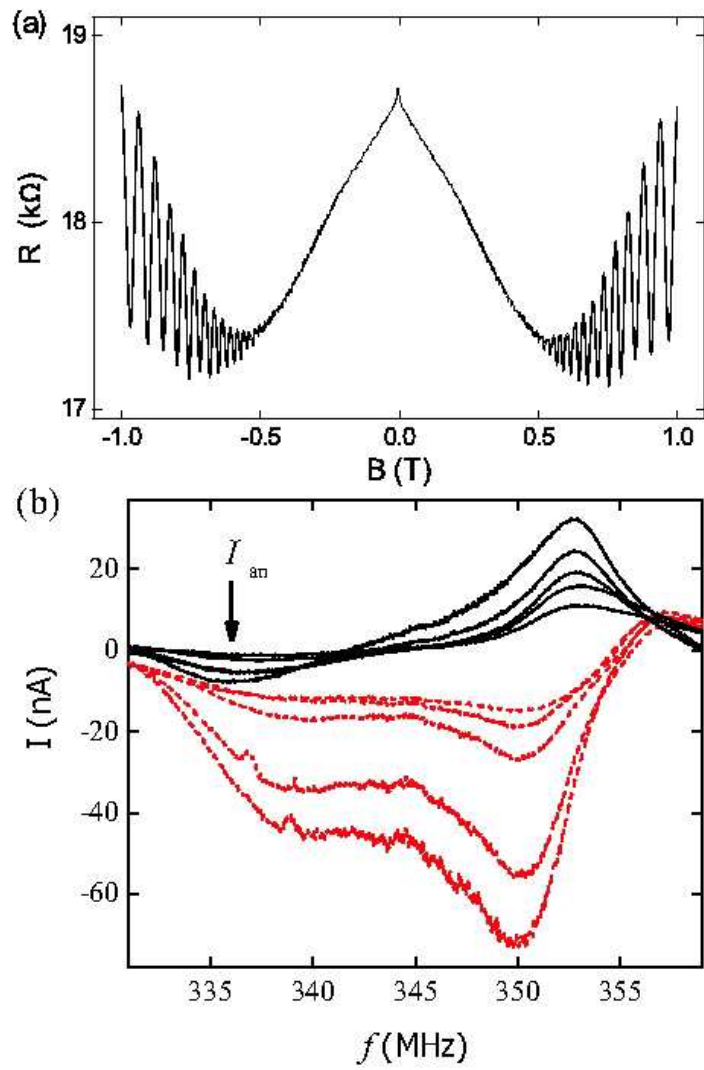
FIG. 2: (a) Characterization of the suspended two-dimensional electron gas: longitudinal magnetoresistance measured in a two point geometry with the Shubnikov-de-Haas oscillations well pronounced. (b) Acoustoelectric current at $T = 1.5$ K with surface acoustic waves driving the current from the left (black) and right (red). The current is measured with a source drain voltage V_{DS} of $50 \mu\text{V}$. At $f = f_{\text{SAW}}$, the IDTs generate acoustical waves and the acoustoelectric current is observed as a dip in the current. The electron gas was tuned into high resistance by applying a backgate voltage ($V_{\text{bg}} \approx 200$ V). Driving an acoustic excitation from the right reverses the sign of the normal acoustoelectrical current I_n (traces are given for different power levels from 0 dBm to 10 dBm). The remarkable feature is the region at the edge of the acoustic bandpass: for both directions of the acoustic excitation the anomalous acoustoelectric current I_{an} shows no sign reversal.

FIG. 3: (a) Standing wave measurements – nonlinear response: the current sensitive to the relative phase shift ϕ is induced by the acoustic standing wave proportional only to the anomalous acoustoelectric current. Shown is the phase shift ϕ between driving signal applied at IDTs left and right for increasing acoustic power. The maximum current appears at 180 deg phase shift. The applied RF power at the IDTs increases from -40 dbm to -10 dBm. (b) The sinusoidal shape evolves into a $(\sin x)/x$ -shape, indicating the shock front. At even larger powers the resonator jumps into the next higher acoustic mode and the sinusoidal wave form reemerges.

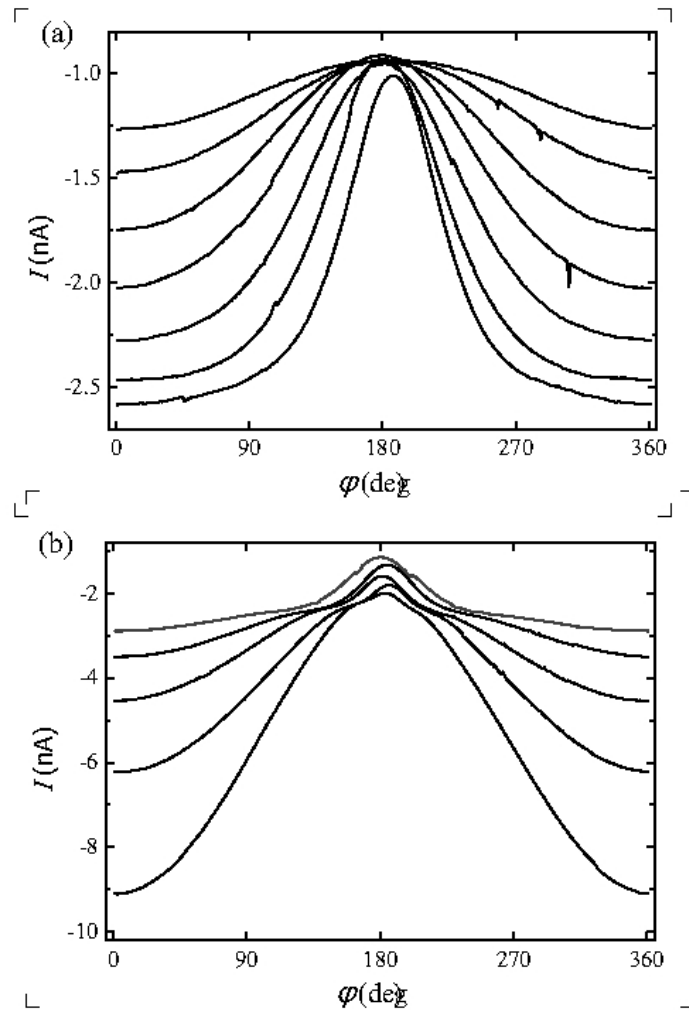
FIG. 4: (a) Full scan of the standing wave measurements: the current sensitive to relative phase shift ϕ is induced by the acoustic standing wave proportional only to the anomalous acoustoelectric current. At large powers the resonator jumps into the next higher acoustic mode and the sinusoidal wave form reemerges. (b) Maximum current vs. applied SAW amplitude and comparison to model calculations: a square dependence on SAW amplitude is observed, whereas for small amplitudes deviations are found. Inset shows the calculated dependence of the current on the phase (see text for details).



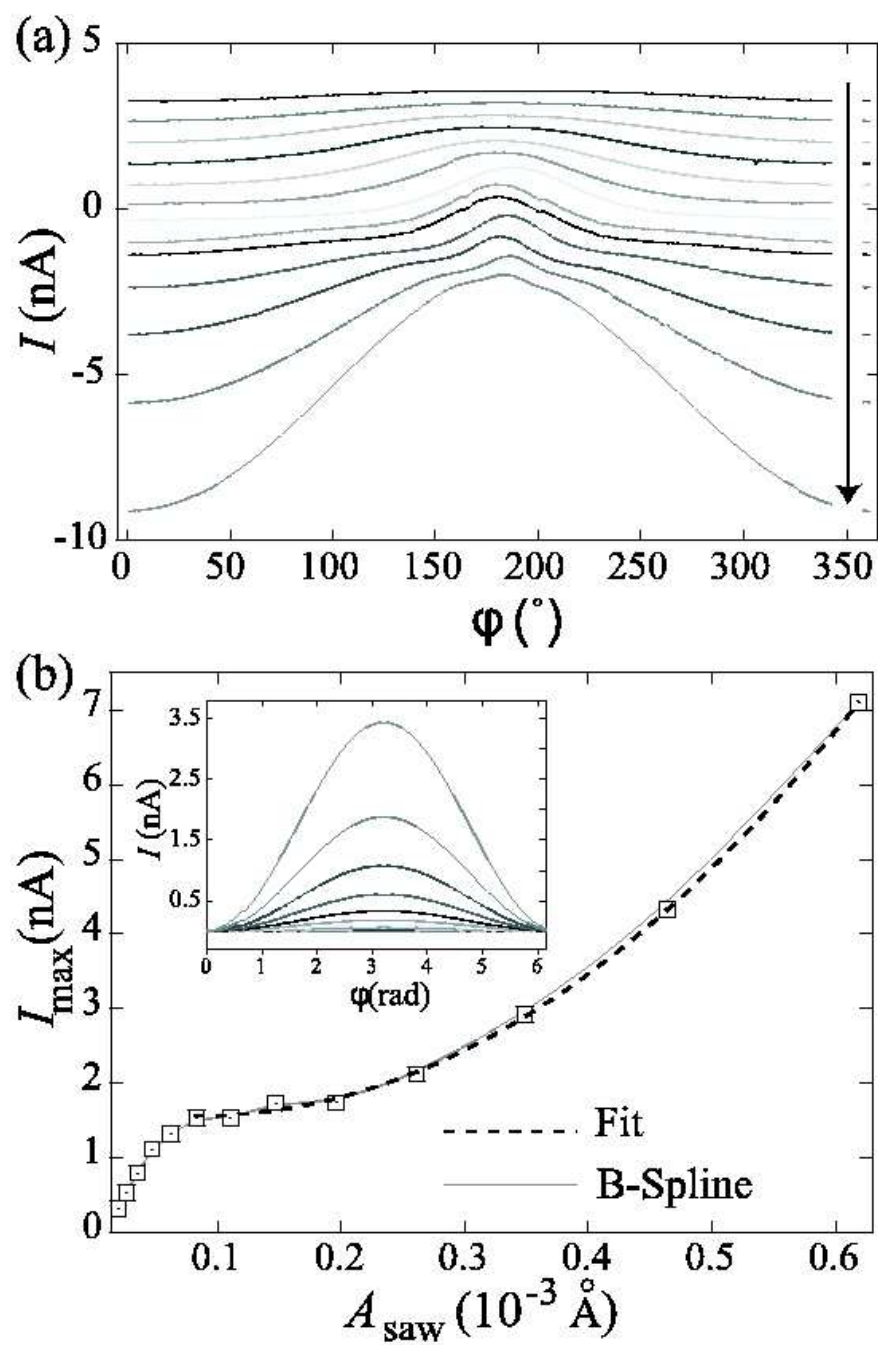
Beil *et al*, Figure 1/4



Beil *et al*, Figure 2/4



Beil *et al*, Figure 3/4



Beil *et al*, Figure 4/4